



AHL Newsletter

AHL Newsletter, Volume 30, Number 2

June 2026

In this issue:

Update from the Director	2
Introducing our new companion animal panels.....	3
New cytology fee structure	4
OAHN June update.....	5
Staff highlights.....	7
Ruminants	
Mycotic abortion in a Holstein cow	8
What is your diagnosis? A liver from a 3-year-old ewe.....	10
Bovine abortion due to BVDV infection	11
Swine	
Update on PEDV and PdCoV detection in Ontario.....	13
Avian/fur/exotic	
Avian metapneumovirus update.....	15
Equine	
Equine herpesvirus -1 abortion in pregnant mare.....	17
Companion animals	
Feline sarcoid	22
Feline hypokalemia and polymyopathy - What is Conn's syndrome?	23
Whole blood arsenic concentrations in cats: A diagnostic challenge	26
Answer	
What is your diagnosis? A liver from a 3-year-old ewe.....	28

AHL Newsletter

March 2026 - Volume 30, Number 2

ISSN 1481-7179

Editor: **Maria Spinato**, DVM, DVSc, Diplomate ACVP, MBA

Editorial Assistants: **Helen Oliver, Sofija Jelacic**

The *AHL Newsletter* is published quarterly (March, June, September, December) by the Animal Health Laboratory, Laboratory Services Division, University of Guelph.

Its mission is to inform AHL clients and partners about AHL current activities, and laboratory-based animal disease events and disease trends. All material is copyright 2025. Ideas and opinions expressed herein do not necessarily reflect the opinions of the University or the editor.

Articles may be reprinted with the permission of the editor and with appropriate credit given to the AHL Newsletter.

Mailing address & contact information:

Animal Health Laboratory

Laboratory Services Division, University of Guelph

Box 3612, Guelph, Ontario, Canada N1H 6R8

Phone: (519) 824-4120 ext. 54538; fax: (519) 821-8072

To receive an **electronic copy of this Newsletter**, please send your email address to us at holiver@uoguelph.ca

Update from the Director



The view from the Director's office

Finally, this long winter is over and spring has (reluctantly) arrived. At the AHL, we have just finished hosting the national Canadian Animal Health Laboratorians Network (CAHLN) conference. This meeting brings together veterinary laboratory workers from across the country, originating from a variety of organizations that include provincial and university diagnostic laboratories, CFIA, veterinary colleges and researchers. It was a great opportunity to network with colleagues and to catch up on the latest technologies (whole genome sequencing, machine learning, artificial intelligence) that will transform the way in which we will work in the coming years. One Health was also a topic of interest at this conference, most especially how to understand and combat misinformation. Many thanks to all the AHL staff who helped to organize the conference and who presented at the meeting!

After 7 years at the helm of AHL, I will be retiring at the end of June. It has been a great pleasure and privilege to work with the incredible group of intelligent and dedicated people here at the AHL. Surviving the COVID years will probably be my most memorable recollection as I look back over my tenure. But we made it through that challenge, and I am confident that the new AHL Director will guide our laboratory successfully as it continues to provide valuable services to the animal health community in Ontario and across Canada.

Thank you for your support of the AHL. Best wishes for an enjoyable summer.

Maria Spinato, Director

Animal Health Laboratory, University of Guelph, Guelph, ON.

Introducing our new companion animal panels

Tim Pasma

Animal Health Laboratory, University of Guelph, Guelph, ON.

AHL Newsletter 2026;30(2):3.

In response to feedback received from clients at our annual AHL Client Feedback meeting and our biennial client survey, we are pleased to offer new panels for diarrhea and respiratory diagnostic testing for canine and feline species.

The canine diarrhea panel (candp) includes testing for: *Campylobacter coli*, *C. jejuni*, *Clostridium difficile* toxins A/B, *Clostridium perfringens* CPA (quantification), CPE (quantification), NetE and NetF toxins, *Salmonella* spp. (centpa1), canine distemper virus (cdvmb), canine parvovirus 2 (pv2mb), canine enteric coronavirus (cecvpcr), *Cryptosporidium* spp. (crypto) and *Giardia duodenalis* (gia).

The feline diarrhea panel (feldp) includes testing for *Campylobacter coli*, *C. jejuni*, *Clostridium perfringens*, CPA (quantification) and CPE (quantification) toxins, *Salmonella* spp. (fentpa1), *Tritrichomonas fetus* (tfpcr), feline panleukopenia (pv2mb), *Cryptosporidium* spp. (crypto), *Giardia duodenalis* (gia) and *Toxoplasma gondii* (toxopcr).

Samples for the diarrhea panels should include 2-3 g of feces or intestinal content split into 3 separate sterile vials for distribution to the lab sections. If splitting of samples is done at AHL, an extra splitting charge will be applied.

The canine respiratory panel (canrp) includes testing for: *Bordetella bronchiseptica*, *Streptococcus equi* ssp. *zooepidemicus* (respa1), canine adenovirus 1/2, canine herpesvirus 1, canine parainfluenza virus (chappcr), canine distemper virus (cdvmb), canine respiratory coronavirus (crecvpcr), influenza A virus matrix PCR (inflpcr) and *Mycoplasma* culture (mculn) (e.g., *M. cynos*, *M. canis*, *M. edwardii*).

The feline respiratory panel (felrp) includes testing for: *Bordetella bronchiseptica*, *Streptococcus equi* ssp. *zooepidemicus* (respa1), feline calicivirus, feline herpesvirus 1 (fcfhpcr), influenza A virus matrix PCR (inflpcr), and *Mycoplasma* culture (mculn) (e.g. *M. felis*, *M.gateae*).

Samples for the respiratory panels can include bronchial lavage, pleural fluid, lung tissue or nasal/respiratory swabs. If submitting fluids, please split into 3 separate sterile vials for distribution to the lab sections; if splitting of samples is done at AHL an extra splitting charge will be applied. For swabs, please submit 2 swabs – an Eswab (not a gel swab) and a virus transport medium swab.

New cytology fee structure

Tim Pasma, Kris Ruotsalo, Marco Leung

Animal Health Laboratory, University of Guelph, Guelph, ON.

AHL Newsletter 2026;30(2):4.

In order to continue providing high-quality cytology services and maintain our turnaround time standards, we have updated our cytology submission guidelines and fee structure. Fees and slide limits are tiered based on the number of sites sampled to ensure billing transparency and streamline our laboratory processing.

Cytology smears

- 1-2 sites: Maximum 5 slides (Testcode: cytsm1)
- 3-4 sites: Maximum 10 slides (Testcode: cytsm2)
- 5-7 sites: Maximum 15 slides (Testcode: cytsm3)
- 8-9 sites: Maximum 18 slides (Testcode: cytsm4)
- 10 sites: Maximum 20 slides (Testcode: cytsm5)

Lymph node and bone marrow

- Lymph node: Maximum 10 slides (Testcode: cytln)
- Bone marrow: Maximum 10 slides (Testcode: bm)

Slides submitted above the maximum limit for each category will result in an additional charge. We highly encourage clinicians to submit only the most representative slides for diagnostic evaluation to avoid unnecessary charges.

Fluid submissions

For general fluid analyses, billing is based on a charge per tube rather than per slide. This applies to abdominal, thoracic, synovial, transtracheal / BAL, and urine samples (Testcode: cyto).

If you submit multiple tubes, for example, a BAL submission, and would like these tubes pooled, please indicate this on the submission form.

Special exception for CSF - (Testcode: cytsf)

Handling protocol: Deliver CSF samples to the laboratory immediately. If the sample cannot be sent immediately, split the sample evenly into two plain tubes: one neat sample and one with an equal volume of autologous serum added to the CSF fluid to preserve cell morphology. Please label both tubes appropriately.

Billing exception: When following this specific preservation protocol, the two submitted CSF tubes will incur only one single charge.



OAHN Update – June 2026

Mike Deane, Tanya Rossi

Animal Health Laboratory, University of Guelph, Guelph, ON.

The Ontario Animal Health Network had a very productive spring, with many of our networks publishing new species-specific reports. At the end of April, we held our OAHN Annual General Meeting (AGM), with our networks presenting their accomplishments over the past year and plans for the year ahead.

OAHN AGM Speaker Series 2026

For the past two years, we have hosted an OAHN speaker series in place of an AGM keynote; the presentations are available to veterinarians and animal health professionals. Additionally, we post these talks online for all of our registered veterinarians and members. This year, we were fortunate enough to have five talks, which are listed below. A heartfelt thanks to the veterinary experts who provided these talks, and to all of the Ontario veterinary professionals who attended. These talks are password protected on the OAHN website, so you need to register and be signed in to view them.

- The ups and downs of HPAI vaccination in France and the Netherlands - Dr. Jean-Pierre Vaillancourt
- Utilizing salivary anti-CarLA IgA testing to manage gastrointestinal parasitism in Ontario sheep - Dr. Brad DeWolf
- Small farms – big opportunities - Dr. Michelle Buckley
- New Insights into Wild Pig Control in Manitoba - Dr. Wayne Lees
- Ontario tick borne diseases to be on the lookout for in 2026 – Lyme is not alone - Drs. Andrew Peregrine and Scott Weese

Watch the presentations here: [OAHN AGM Speaker Series 2026](#)

OAHN Bovine Project: Investigation of *Mycoplasma wenyonii* and *Candidatus Mycoplasma haemobos* in Ontario dairy cattle

The recently completed OAHN bovine network project was a pilot study of blood samples collected from Ontario dairy cattle to determine whether *M. wenyonii* and *C. M. haemobos* are present in Ontario dairy herds, and to explore potential herd-level risk factors. In addition to the project report, the

network also created a summary document: Tips for Testing Cattle for *Mycoplasma wenyonii* and *Candidatus Mycoplasma haemobos*. Both of these documents can be accessed here: [Project Report: Investigation of *Mycoplasma wenyonii* and *Candidatus Mycoplasma haemobos* in Ontario dairy cattle](#)

New Reports

These are the most recent reports published by OAHN. We publish regularly, so be sure to check back in between newsletters to see what's new. To view any of the veterinary reports below, please click on the link for each report, or go to OAHN.ca and navigate to the species in which you are interested.

Bovine Network - [Nov 2025 – Jan 2026 Vet Report](#)

- Surveillance updates
- Q4 Bovine data from AHL
- OAHN data summary: Dairy & Beef respiratory testing results 2021-2025
- Mastitis pathogens from milk cultures submitted to AHL in 2025
- *Salmonella* Dublin 2025

Poultry Network - [Dec 2025 – Feb 2026 Vet Report](#)

- Reovirus, infectious bronchitis virus (IBV), infectious bursal disease virus (IBDV), avian metapneumovirus (AMPV), and fowl adenovirus (FAdV, IBH) strains in Ontario from January 1st, 2023, to December 31st, 2025
- Poultry veterinary survey highlights - Q1 2026

Staff highlights



Dr. Emily Brouwer has been accepted as a Founding Fellow of the American College of Veterinary Pathology (ACVP) Veterinary Forensic Pathology Fellowship Program.

The veterinary forensic pathology fellowship program is supported by the ACVP to fulfill the need to train pathologists in medicolegal death investigation and forensic science. The initiative was brought forward by a founding fellow review committee- six experts in the field- who review applications from ACVP diplomates to become 'founding fellows'. There are currently 14 ACVP diplomates who have been accepted as founding fellows.

Congratulations on this momentous achievement Emily!



Dr. Maria Spinato has been awarded the prestigious 2026 Laboratorian of the Year Award by the Canadian Animal Health Laboratorians Network (CAHLN). This award is bestowed on an outstanding individual who has made a significant contribution to animal health laboratory medicine in Canada.

Congratulations Maria!

RUMINANTS

Mycotic abortion in a Holstein cow

Meegan Larsen

Animal Health Laboratory, University of Guelph, Guelph, ON.

AHL Newsletter 2026;30(2):8.

A clinically healthy, first lactation heifer aborted at approximately 200 days in calf. Multiple late term abortions had occurred on the farm over the previous 6 months. The fetus and a small piece of placenta, including two cotyledons, were submitted to the AHL for postmortem examination. The skin of the eyelid of the fetus was roughened and there was thickening of the intercotyledonary placenta. The most significant microscopic finding was a necrotizing placentitis with numerous intralesional fungal hyphae (**Fig. 1**). The roughened fetal eyelid skin corresponded to an area of epidermal hyperkeratosis with intracorneal pustules (**Fig. 2**). Eyelid pustules are often a feature of mycotic placentitis; however, no hyphae were observed in this case. There was also a mild suppurative and histiocytic fetal pneumonia. Collectively, the histologic lesions were diagnostic for mycotic abortion, and this diagnosis was confirmed by the visualization of fungal hyphae on a placental wet mount. No concurrent bacterial or viral causes of abortion were identified via bacterial culture or PCR testing.

Mycotic abortion in cows is generally caused by *Aspergillus fumigatus* or *Mucor* species of fungi. It occurs due to ingestion or inhalation of spores from moldy feed or bedding, followed by hematogenous spread to the uterus and placenta. This infection is associated with sporadic, usually mid-late term abortions in a herd. The incidence is highest between November and April, likely due to confinement and high-density housing over the winter. The dam often does not show signs of illness prior to or after the abortion, but retained placenta is relatively common.

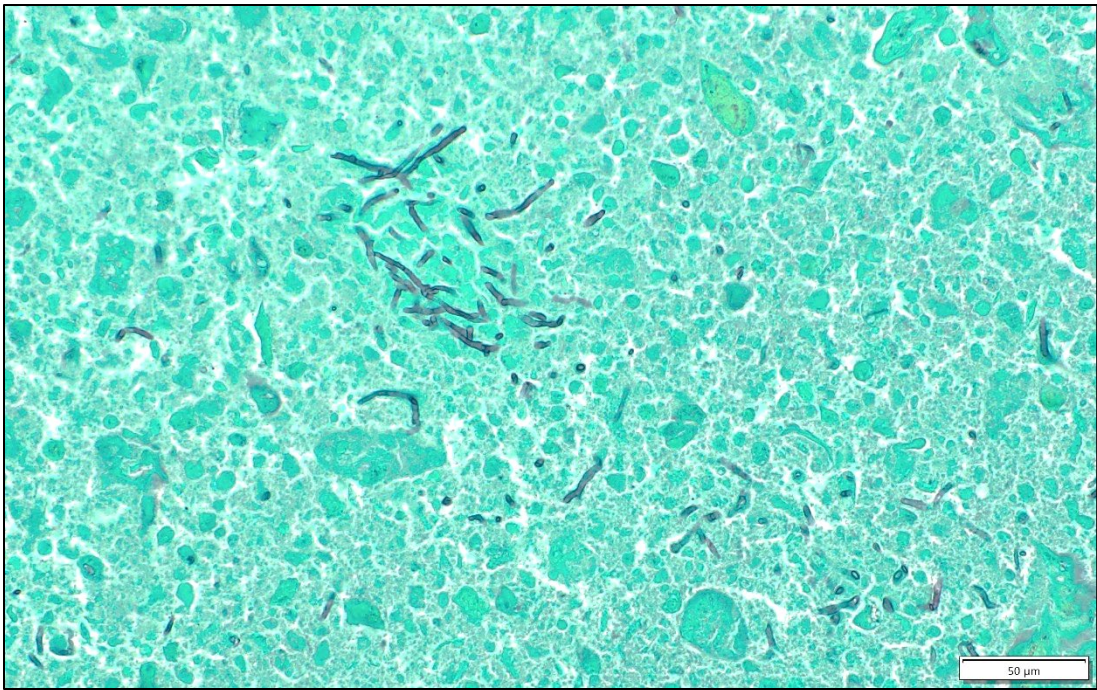


Figure 1. Placental necrosis with numerous fungal hyphae stained black. GMS stain.

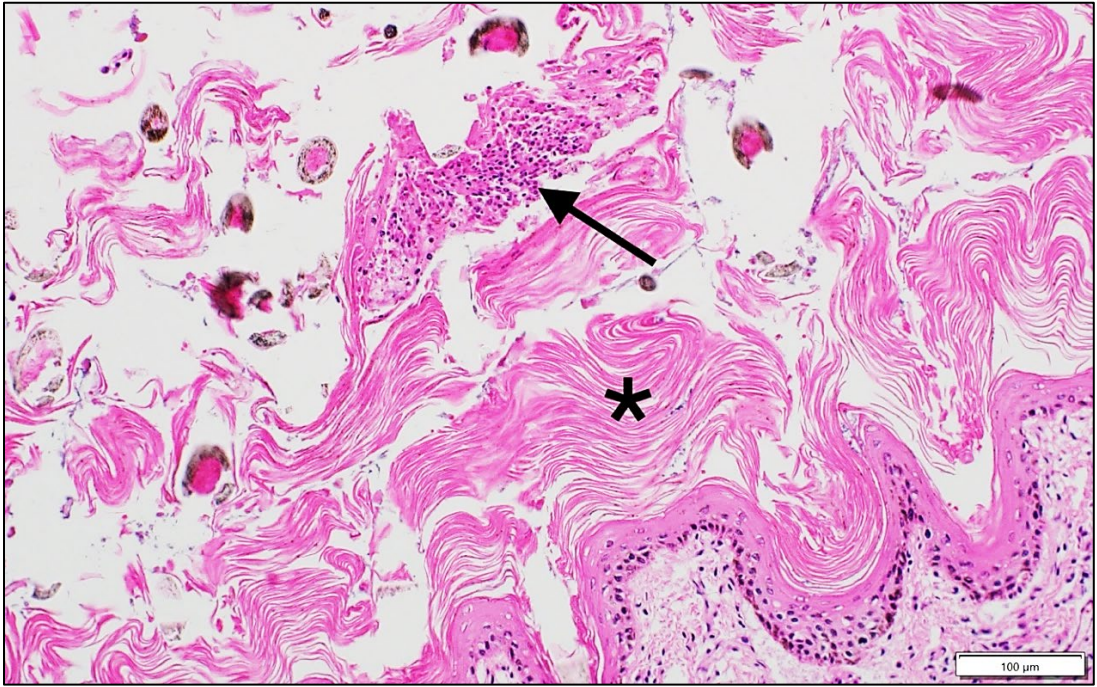


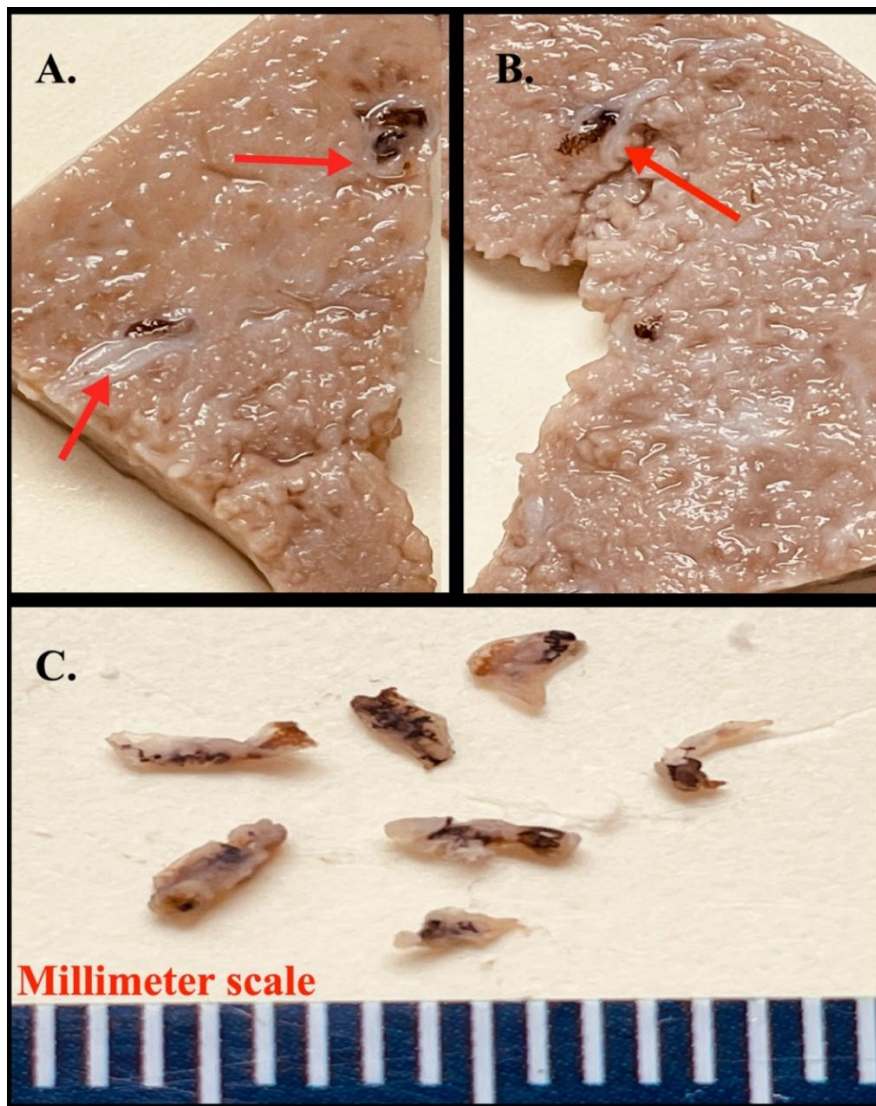
Figure 2. Excess lamellar keratin on the epidermal surface of the eyelid (*) with a pustule (arrow).

What's your diagnosis? Liver from a 3-year-old ewe

Amanda Mansz

Animal Health Laboratory, University of Guelph, Guelph, ON.

AHL Newsletter 2026;30(2):10.



Figures A. & B. Formalin-fixed liver tissue from a 3-year-old ewe. Red arrows indicate bile ducts with periportal fibrosis and black-brown pigmentation. **Figure C.** Organisms retrieved from bile duct lumens.

Refer to last page for the answer.

Bovine abortion due to BVDV infection

Dominique Comeau

Animal Health Laboratory, University of Guelph, Guelph, ON.

AHL Newsletter 2026;30(2):11.

A Holstein calf and associated amnion were submitted to the Animal Health Laboratory as part of an investigation into an abortion storm. The farm had multiple abortions as well as multiple live calves which were born several weeks premature. On postmortem examination, there were minimal abnormalities in the fetus which had a crown rump length and other fetal characteristics consistent with a gestation age of approximately 8 months (full term). The amnion was diffusely edematous, with patchy pale yellow to brown discoloration consistent with meconium staining. Meconium staining is a nonspecific finding related to fetal stress.

Histologically, there was extensive effacement of the cardiac muscle by fibrosis with lymphocytic inflammation primarily focused along the epicardium (**Fig 1**). This inflammation extended into the myocardium and also involved the endocardium. There was also moderate lymphoid atrophy throughout the thymus (**Fig 2**). These histologic lesions are supportive of bovine viral diarrhea virus (BVDV) infection. Testing of the fetal tissues detected BVDV by PCR with a Ct value between 30 and 32.

BVDV is a well-known cause of bovine abortion, infertility, and early embryonic loss, as well as severe systemic disease presentations such as mucosal disease. However, detection of this agent has been uncommon in abortion submissions to the AHL. In review of abortion submissions in the last ten years (approximately 1079 cases), there were only seven cases in which the cause was diagnosed as BVDV (0.65 %). One case was identified in 2016, two cases from the same abortion outbreak on one farm in 2017, one case in 2018, and two cases in 2026. For 2026, in addition to the above-described case, another farm with a history of multiple abortions had a submitted fetus test positive for BVDV. There were no supportive histologic lesions noted in this second case, although detection of BVDV from fetal tissues by PCR was still considered significant.

In North America, control of BVDV has primarily focused on vaccination. Vaccination of heifers and cows against BVDV reduces the risk of fetal malformations and abortions, as well as reducing the risk of having persistently infected calves born on farm. These PI animals are immunotolerant to BVDV and persistently shed virus into the environment, acting as a major source of infection on farm. Therefore, prevention of PI animals is a large part of control by vaccination. **In this case, the affected herd was not vaccinated for BVDV.** This highlights that despite the low prevalence of confirmed cases of BVDV, vaccination against this agent remains an important part of bovine herd health and disease prevention.

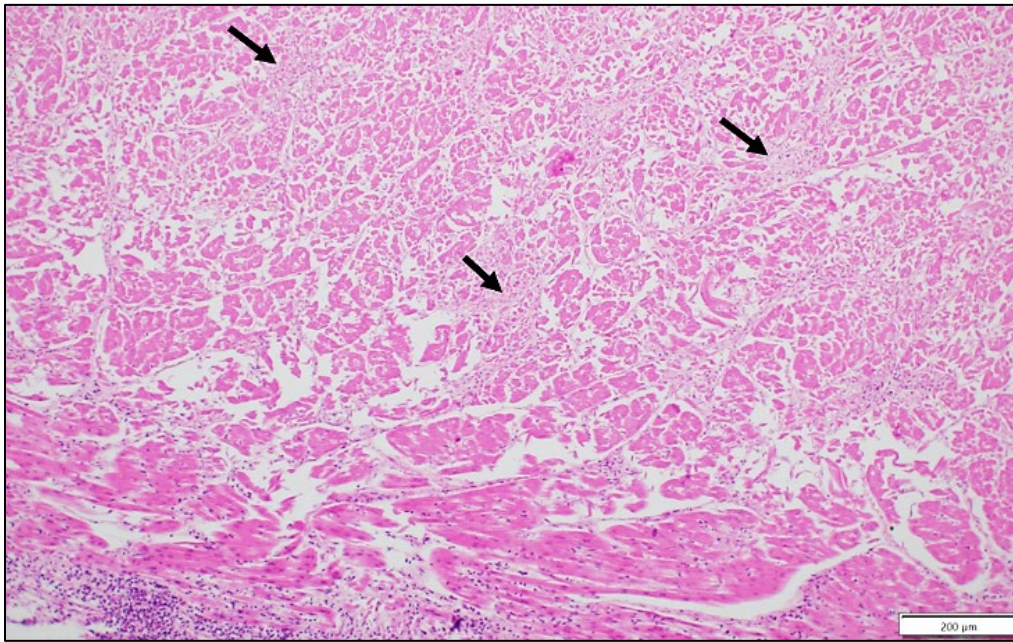


Figure 1: A photomicrograph of the fetal heart showing areas of fibrosis (arrows) and lymphocytic inflammation in the epicardium (bottom left). H&E stain, 400X.

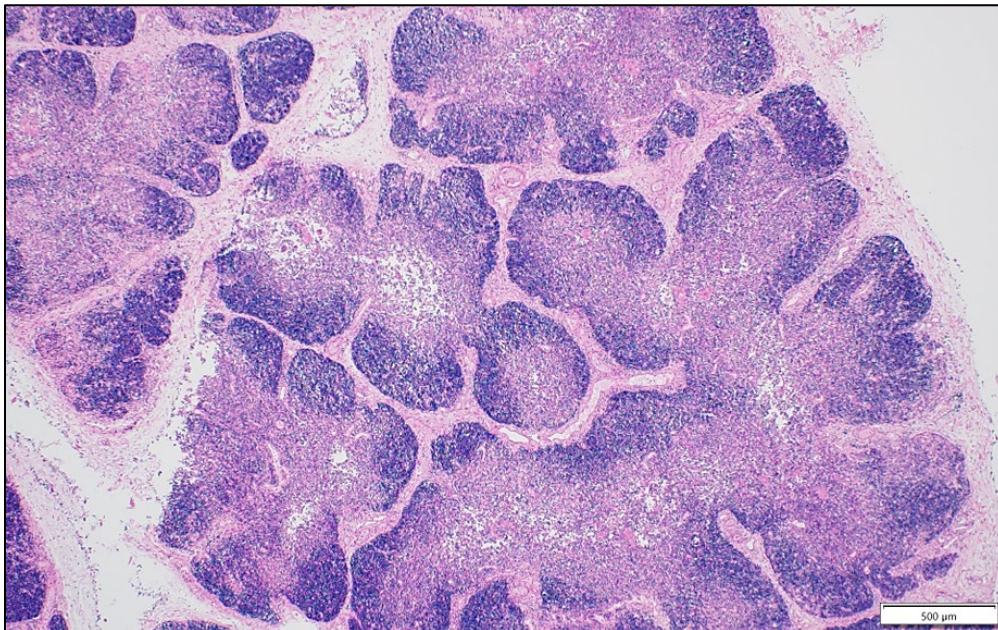


Figure 2: A photomicrograph of the fetal thymus showing significant reduction in the lymphocyte population (blue areas) with a relative increase in the medullary tissue (pink areas). H&E stain, 200X.

Reference

1. Newcomer BW, et al. Efficacy of bovine viral diarrhea virus vaccination to prevent reproductive disease: A meta-analysis. *Theriogenology*. 2015;83(3):360-365. <https://doi.org/10.1016/j.theriogenology.2014.09.028>

SWINE

Update on porcine epidemic diarrhea virus (PEDV) and porcine deltacoronavirus (PDCoV) detection in Ontario

Davor Ojkic, Tanya Rossi, Rebecca Egan

Animal Health Laboratory, University of Guelph, Guelph, ON.

AHL Newsletter 2026;30(2):13.

In late 2025 and early 2026, there was a spike in the number of cases of porcine epidemic diarrhea virus (PEDV) in Ontario, as reported by Swine Health Ontario (SHO), with a range of 20 to 34 new cases per month from December to February. During that same time, there were also several porcine deltacoronavirus (PDCoV) detections, ranging from 1 to 6 new cases per month. The AHL PCR data reflects this recent increase, with a total of 122 PEDV-positive submissions and 22 PDCoV-positive submissions so far this year. Over the last 5 years, the number of PEDV-positive submissions at the AHL has increased annually, and the number of PDCoV-positive submissions has also been trending upward over this period (**Table 1**).

Table 1. Annual PCR-positive submissions for PEDV and PDCoV at AHL*.

Year	PEDV	PDCoV
2021	42	23
2022	61	29
2023	67	43
2024	100	88
2025	102	65
2026+	122	22

**Multiple submissions per premises, generated by testing for clinical disease and/or monitoring, accounts for a higher number of PCR-positive submissions than total reported positive cases in Ontario*

+ Partial year consists of Jan-May submissions

PEDV spreads rapidly and illness is characterized by a sudden onset of profuse watery diarrhea in nursing piglets, accompanied by vomiting and rapid dehydration with high morbidity and mortality rates. In nursery pigs, morbidity rates can be high, but with less severe diarrhea, dehydration, lethargy, and reduced feed intake, and lower mortality rates. In grower-finisher barns, animals may present with anorexia, lethargy, and less severe diarrhea, but death is uncommon. This disease has a major economic impact due to high neonatal mortality, reduced nursery and finishing performance, and increased labour and treatment costs contributing to financial losses. The clinical signs associated with PDCoV infection are indistinguishable from those of PEDV, but illness and impact tend to be less severe overall.

Movement of infected pigs and transport contamination appear to have been the main causes of disease spread, and this highlights the importance of continued vigilance and strong farm biosecurity, including adequate decontamination of all vehicles (transport trailers, feed delivery trucks, etc). For more

information regarding ongoing PEDV and PDCoV tracking in Ontario, visit the Swine Health Ontario website: <https://www.swinehealthontario.ca/Disease-Information/PED-PDCoV-Tracking-Map>.

References

1. Saif LJ, Wang Q, Vlasova AN, Jung K, Xiao S. Coronaviruses. In: *Diseases of Swine*, 12th ed. Zimmerman JJ, Karriker LA, Ramirez A, Schwartz KJ, Stevenson GW, Zhang J, eds. Wiley-Black Sons; 2026. p 564-574.
2. Swine Health Ontario. <https://www.swinehealthontario.ca> Accessed May 13, 2026.

Avian metapneumovirus update

Andrew Brooks, Tanya Rossi, Emily Martin, Davor Ojkic

Animal Health Laboratory, University of Guelph, Guelph, ON

AHL Newsletter 2026;30(2):15.

Since the detection of avian metapneumovirus (aMPV) in Ontario during the winter of 2024, cases in commercial poultry have continued to be identified through 2025 and into 2026 (**Fig. 1**). A review of laboratory submissions up to May 21, 2026 identified 232 PCR-positive submissions in turkeys and chickens. Most detections were subtype B (approximately 92%), with subtype A accounting for about 8% of cases. Cases in turkeys primarily involved meat birds, whereas infections in chickens were predominantly identified in broiler breeder flocks, with occasional detections in broilers and layers.

Subtype B was also identified in a single gamebird submission and one small flock. Subgroup C has not been detected in commercial poultry to date. However, surveillance confirms the virus is maintained in the region's wildlife reservoir. Subgroup C was first identified in wild waterfowl in Ontario in 2016, and its continued circulation in the province was recently re-confirmed through a targeted waterfowl surveillance program in 2024.

Live aMPV-A vaccines became available in the second half of 2025. Because standard PCR testing alone does not distinguish between vaccine and wild-type field strains, any positive aMPV-A results recorded in late 2025 and 2026 may reflect detection of the vaccine virus rather than a field infection. Genotyping assays are available to differentiate between field strains and vaccine strains.

Clinically, aMPV infection causes respiratory and reproductive disease, with severity and signs that vary by species. In turkeys, the disease may be more pronounced, with high morbidity and clinical signs such as nasal discharge, swollen infraorbital and periorbital sinuses, conjunctivitis, and reduced egg production. In chickens, clinical signs and lesions (**Fig. 2**) often include swelling and subcutaneous edema of the head (“swollen head”), sinusitis, tracheitis, as well neurologic signs such as torticollis or stargazing due to inflammation of the middle or inner ear. Secondary bacterial infections are common and exacerbate clinical disease.

From a diagnostic perspective, aMPV infection can be challenging to confirm because the virus may only be present in the upper respiratory tissues for approximately 6–7 days post-infection. Timing of sampling early in the course of infection is therefore important, ideally selecting multiple acutely affected birds for testing. PCR tests may be performed on swabs of oculo-nasal discharge, the choanal opening, the nasal sinuses and the trachea. Postmortem examination and histopathology may provide supportive findings but are not definitive. Combining PCR with antibody detection (ELISA) can improve case identification, particularly when infection is no longer detectable by PCR. Continued surveillance, prompt diagnosis, and strong biosecurity and flock management remain essential for controlling aMPV in poultry.

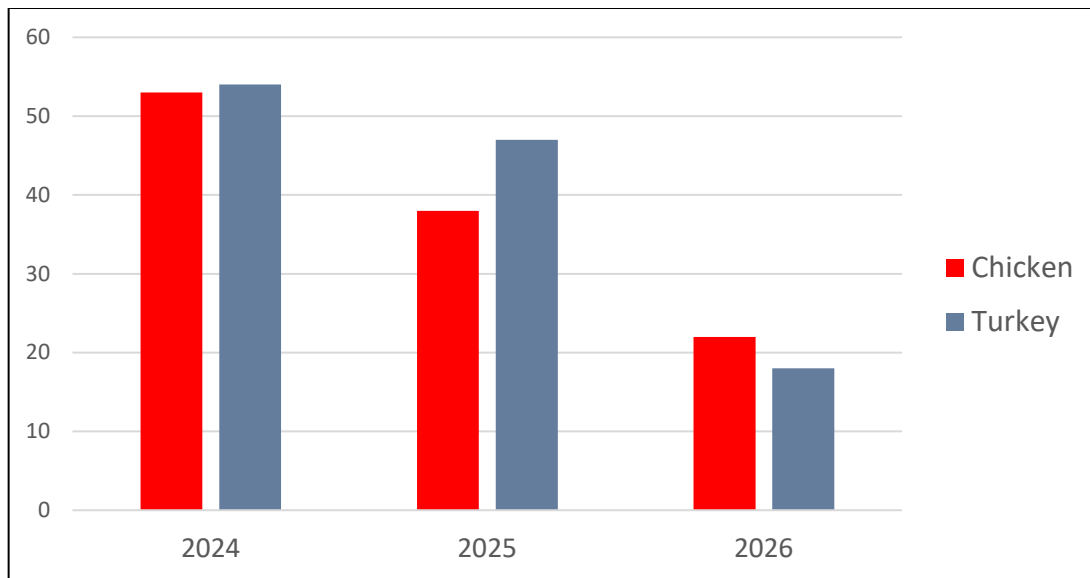


Figure 1. AHL submissions positive by PCR for avian metapneumovirus. Cases continue to be detected in poultry flocks, predominantly involving aMPV subtype B in meat turkeys and broiler breeder chickens.

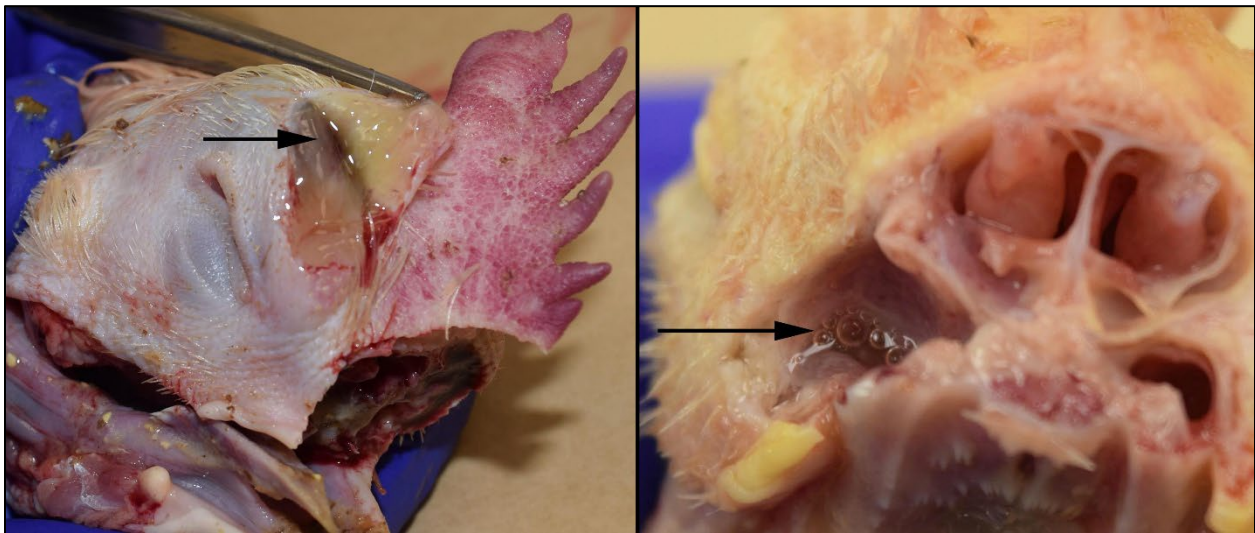


Figure 2. Avian metapneumovirus infection in chickens often produces marked swelling of the head due to subcutaneous edema (left) and sinusitis with discharge that may be clear, mucoid or turbid (right).

References

1. Martin E. Avian metapneumovirus subtype B: First cases confirmed in Canada. AHL Newsletter 2024;28(2):17.
2. Jardine CM, Parmley EJ, Buchanan T, Nituch L, Ojkić D. Avian metapneumovirus subtype C in wild waterfowl in Ontario, Canada. *Transbound Emerg Dis.* 2018 Aug;65(4):1098-1102.
3. Rautenschlein S. Avian metapneumovirus. In: *Diseases of Poultry*, 14th ed. Swayne DE, ed. Wiley Blackwell, 2020; vol 1:135-143.

HORSES

Equine herpesvirus-1 abortion in a pregnant mare

Heindrich N. Snyman, Tanya Rossi

University of Guelph, Animal Health Laboratory

AHL Newsletter 2026;30(2):17.

A multiparous (4th parity) Percheron draught mare suddenly aborted one morning. The mare was in late gestation (~ 305 days) and did not exhibit any obvious premonitory clinical symptoms at the time or within the days leading up to the abortion. During pregnancy, the mare had both outside and inside stable access with an artificial total light time of approximately 16 hours per day. Core vaccines (tetanus, rabies, West Nile virus, and Eastern/Western equine encephalomyelitis virus) were up to date, and the mare received a formulated diet including dry hay, whole oats, mineral, omega 3, microbinder, and a salt additive.

The aborted fetus and whole placenta were submitted for postmortem evaluation and diagnostic testing at the Animal Health Laboratory. On postmortem examination, the crown-rump-length (116.0 cm), umbilical length (71.0 cm), and number of umbilical twists (three and a half loose twists) were all within normal limits, and the fetus was normally formed with adequate joint mobility and normal limb positioning. The placenta was diffusely congested and contained a few indistinct scattered petechial hemorrhages along the allantochorionic surface, with small amounts of enclosed blood-tinged fluid. A single 11.5 cm curvilinear tear was present within the region of the cervical star. Examination of the fetus revealed lungs that were uniformly dark pink-red and rubbery, and samples sank when placed in formalin. The spleen was congested and meaty, and the liver was diffusely dark brown and congested. There was a small volume of tan mucoid gastric and intestinal content, and large amounts of normal olive-green pasty meconium within the colonic loops. The external and internal umbilical arteries and vein all appeared unremarkable.

Although these changes were relatively non-specific, the presence of petechial hemorrhages within the placenta and congestive splenomegaly were suggestive of antigenic stimulation and immune activation, and a potential infectious cause was considered. The changes in the lung could at least partially be ascribed to non-aerated fetal lung, but the increased rubbery consistency also suggested at least some inflammatory infiltrate, although this could simply have been due to fetal stress and meconium aspiration syndrome. The fetus and placenta were routinely sampled for histological evaluation, while pooled fetal and placental tissues were submitted for viral PCR testing (equine adenovirus and equine herpesvirus-1&4, and EHV-2&5).

On histological examination, the thymus, and to a lesser extent the spleen, contained scattered foci of acute fibrinous necrosis and karyorrhectic lymphocytes with acute interstitial hemorrhage (**Fig. 1**). Consistent with meconium aspiration syndrome, the pulmonary alveolar spaces were filled with fibrillar eosinophilic fluid with small to moderate numbers of clustered free-floating macrophages, fewer neutrophils, and large clumps of aspirated keratinized squamous epithelial cells and meconium

Alveolar septa were hypercellular and alveolar spaces also often contained sloughed pyknotic to often fragmented alveolar pneumocytes that rarely contained small bright eosinophilic intranuclear inclusions that subtly margined the nuclear chromatin. Bronchial and bronchiolar epithelium was intact with retained cilia and similar eosinophilic intranuclear inclusions were present (**Fig. 2**). The liver contained few small foci of acute hepatocellular degeneration with loose infiltrates of macrophages, fewer lymphocytes, and rare neutrophils (**Fig. 3**). Small numbers of the same mixed inflammatory cell infiltrates were also present within the pericholangiolar portal tracts. Other than vascular congestion, the placenta appeared histologically unremarkable.

PCR testing of the pooled fetal tissues samples was positive for EHV-1&4 and negative for both EHV-2&5 and equine adenovirus. Additional PCR testing further differentiated the strain as a non-neuropathogenic EHV-1 strain.

While EHV-1 is often better known as a respiratory pathogen or as a cause of neurological and ocular disease in horses, it also represents a major cause of late-term pregnancy loss and abortion in mares. EHV-1 is an alphaherpesvirus and infects horses worldwide. The virus typically infects the respiratory epithelium, and following the establishment of a leukocyte-associated viremia, it localizes in the uterus and placenta, leading to fetal infection and death. Abortions usually affect mares in the last/third trimester and although mares may exhibit mild respiratory symptoms, nasal discharge, or fever, abortions often occur suddenly without any premonitory signs. Placental lesions are usually subtle or absent, and in addition to placental edema and congestion, some cases may exhibit overt placental necrosis. Fetal lesions may also be subtle but when more profound, characteristic lesions include multifocal petechial hemorrhages and necrosis throughout the lungs, liver, spleen, thymus, and lymph nodes, and fetal icterus. Histologically, foci of necrosis often contain epithelial cells with characteristic eosinophilic intranuclear herpesviral inclusions.

Over the past 10-year period of equine abortion submissions to the AHL, equine herpesvirus-1 was implicated as the cause for abortion in a total of 30 cases (**Table 1**). The annual incidence varied between 0 to 7 cases per year, with a peak in the 2020 and 2021 years and no detected cases in 2023. 27 cases were submitted as full diagnostic work-ups that included a combination of postmortem, histology, bacteriology, and PCR testing, while two cases were based on histological lesions and confirmatory immunohistochemical (IHC) staining for EHV-1. A single case was suspected based on characteristic postmortem lesions, but was not further confirmed by molecular testing or IHC. Both neuropathogenic and non-neuropathogenic EHV-1 strains were implicated, with non-neuropathogenic strains (16) outnumbering neuropathic strains (11).

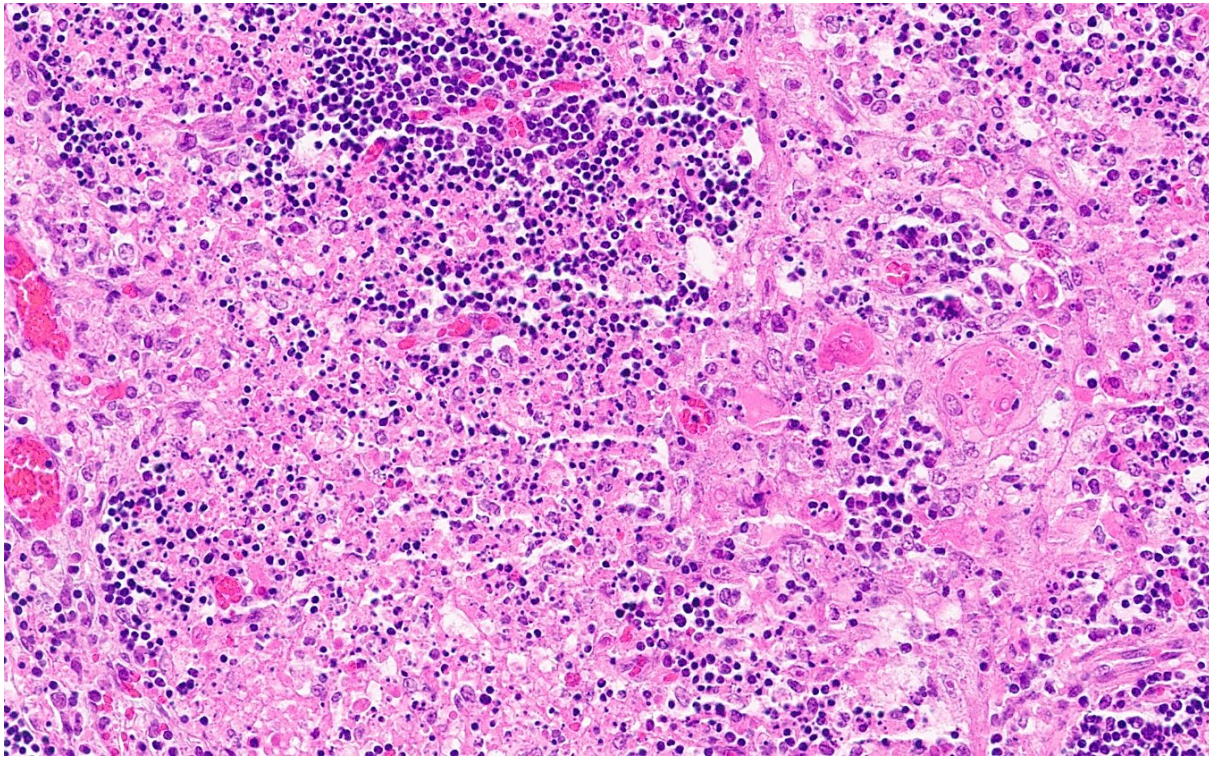


Figure 1. Histological findings in an aborted fetus infected with non-neuropathogenic equine herpesvirus-1. Thymus with foci of acute fibrinous necrosis, lymphocyte karyorrhexis and acute interstitial hemorrhage. H&E stain.

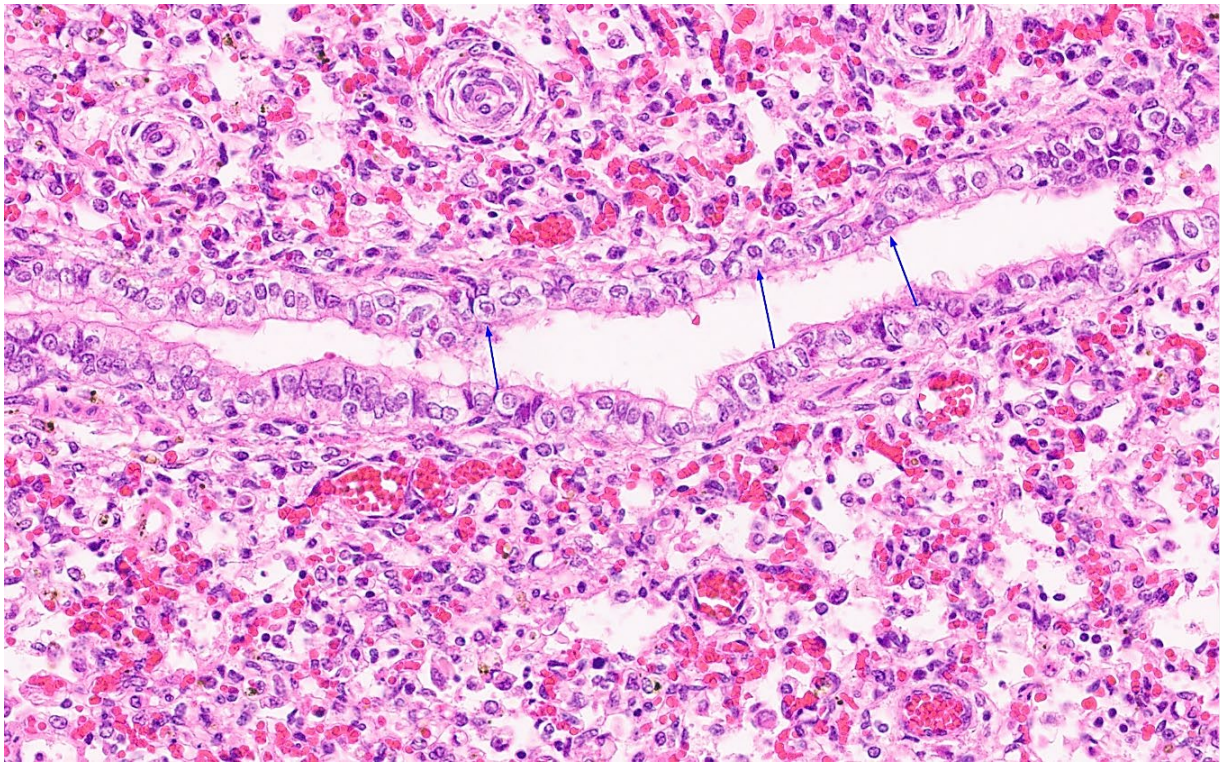


Figure 2. Histological findings in an aborted fetus infected with non-neuropathogenic equine herpesvirus-1. A few bronchiolar epithelial cells contain an eosinophilic intranuclear viral inclusion body with margined chromatin (arrows). H&E stain.

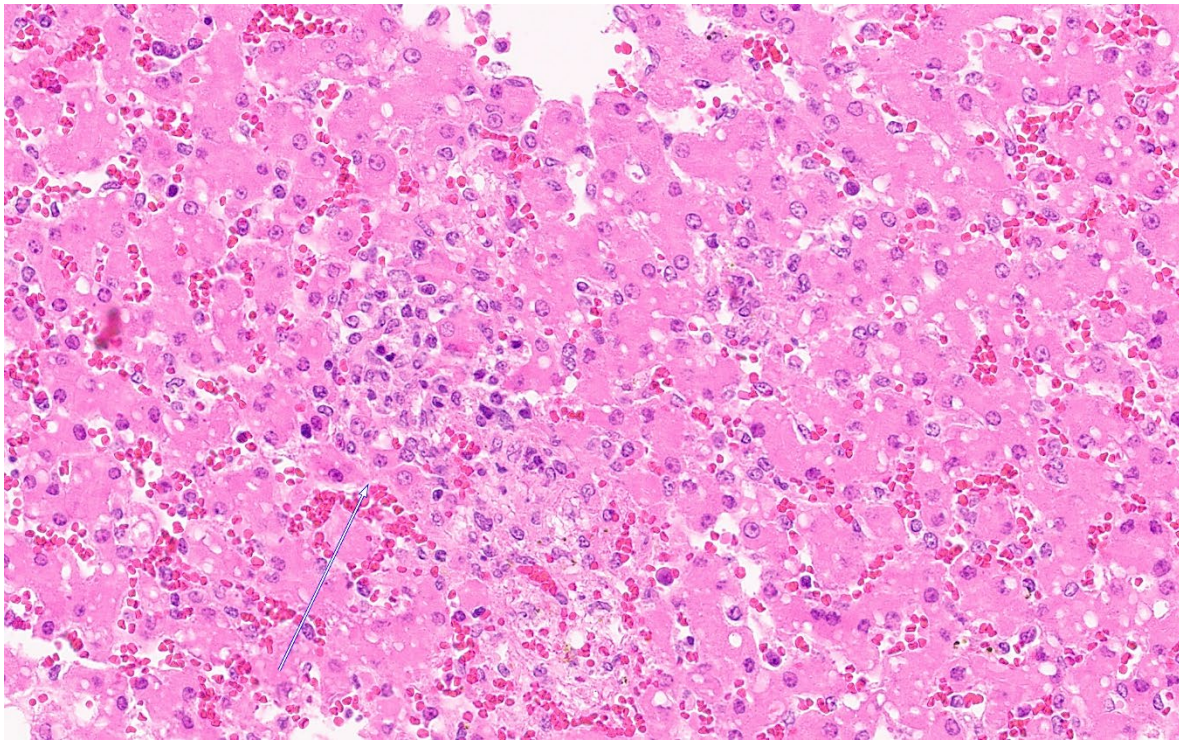


Figure 3. Histological findings in an aborted fetus infected with non-neuropathogenic equine herpesvirus-1. The liver contains few small foci of acute hepatocellular degeneration with loose infiltrates of macrophages, fewer lymphocytes, and rare neutrophils (arrow). H&E stain.

Table 1. Equine abortion submissions to the AHL over a 10-year period (Jan 2016- May 2026). 2017 and 2021 each contained a single case where EHV-1 abortion was diagnosed based on histology and IHC staining, and in 2019, a single case was diagnosed based on characteristic postmortem findings.

Year	Cases
2016	1
2017	4
2018	3
2019	4
2020	7
2021	5
2022	2
2023	0
2024	2
2025	1
2026	1
Sum:	30

References

1. Soboll-Hussey G, et al. Relationship between equine herpesvirus-1 viremia and abortion or equine herpesvirus myeloencephalopathy in domesticated horses: A systematic review. *J Vet Intern Med.* 2023 Dec 9;38(3):1872–1891.
2. Pronost S, et al. Neuropathogenic and non-neuropathogenic variants of equine herpesvirus 1 in France. *Vet Microbiol.* 2010 Oct 26;145(3-4):329-33.
3. <https://www.merckvetmanual.com/respiratory-system/respiratory-diseases-of-horses/equine-herpesvirus-infection>

COMPANION ANIMALS

Feline sarcoid

Siobhan O'Sullivan

Animal Health Laboratory, University of Guelph, Guelph, ON

AHL Newsletter 2026;30(2):22.

A 1.5-year-old domestic short-haired cat presented with a small 1.0 cm red growth on the muzzle adjacent to the nares. Histopathology revealed an infiltrative mesenchymal mass composed of densely arranged spindle cells in a fine collagenous matrix. There was 2-fold anisokaryosis and 4 mitotic figures in ten high power fields (400x/2.37 mm²). The epidermis contained few elongate rete pegs. This presentation was considered most compatible with feline sarcoid.

Feline sarcoid, also known as cutaneous fibropapilloma, is an uncommon feline tumour. It tends to occur in young cats, generally on the face, but has been reported in other locations. Bovine papillomaviruses (BPV-14) have been causally linked to feline sarcoid; therefore, cats in rural areas tend to be more at risk. Due to their infiltrative nature and potential for recurrence, wide surgical resection of feline sarcoids is recommended; however, this is often limited by the tumour's location. Metastasis has not been documented.

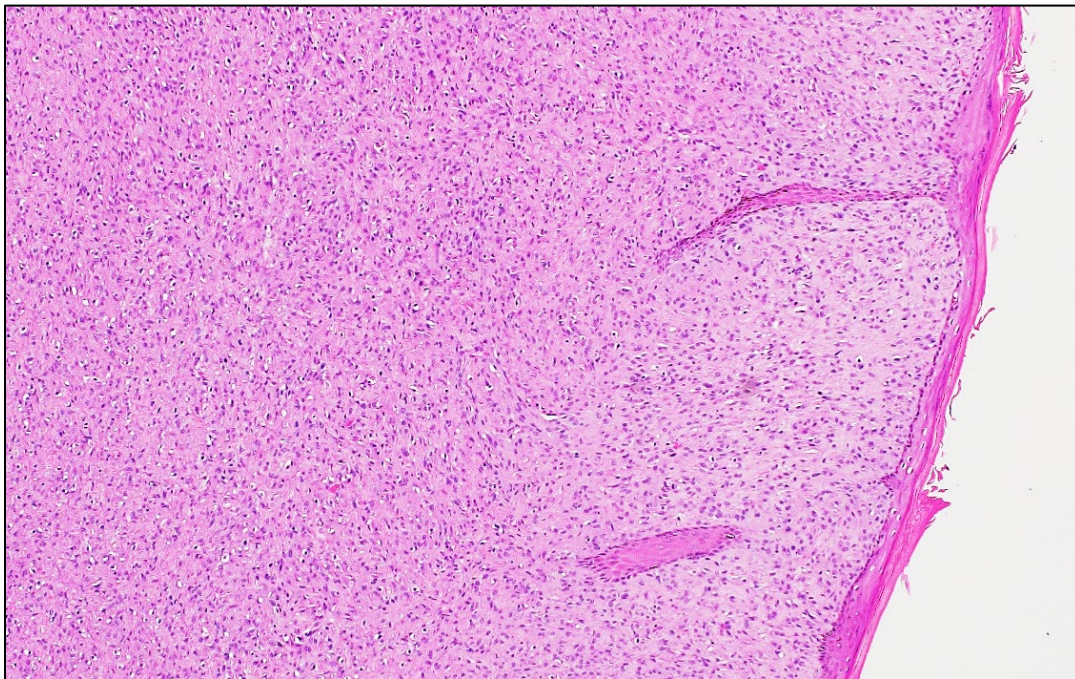


Figure 1. Feline, skin. A mesenchymal mass composed of densely-arranged spindle cells in a fine collagenous matrix. There are few elongate rete pegs in the epidermis. H&E stain.

References

1. Wood CJ, et al. Biological behaviour and clinical outcome in 42 cats with sarcoids (cutaneous fibropapillomas). *Vet Comp Oncol.* 2020;18(4):699-705.
 2. Greenwood S, et al. Oral sarcoid in a cat. *Can Vet J.* 2019; 60(5):485-489.
-

Feline hypokalemia and polymyopathy ... What is Conn's syndrome?

Amanda Mansz

Animal Health Laboratory, University of Guelph, Guelph, ON

AHL Newsletter 2026;30(2):23.

A 14-year-old male neutered cat was submitted to the AHL for postmortem examination following euthanasia with a clinical history of drooling, flaccid paraparesis of all four limbs with muscle tremors, and low serum potassium (2.3 mmol/l; ref 3.4 – 5.3). There was a mild increase in glucose and ALT; however, all other biochemical parameters were within reference range.

Postmortem examination revealed neoplasia of the right adrenal gland, surrounded by mild hemorrhage. There was no distinguishable adrenal cortex or medulla, and the entire gland was replaced by a 2.5 cm x 2.0 cm x 1.1 cm soft, marbled light yellow to tan, encapsulated, rounded mass (**Fig. 1**).

Microscopic examination highlighted virtually complete obliteration of the normal adrenal gland parenchyma by an expansile nodule of highly vacuolated polygonal cells, resembling epithelial cells of the adrenal cortex (**Fig. 2**). The neoplastic cells focally invaded through the adrenal capsule (**Fig. 2b**). The left adrenal gland showed a thinned cortex (contralateral adrenal cortical atrophy) (**Fig. 2d**). Based on the combination of the clinical findings, gross and microscopic findings, a functional, aldosterone secreting adrenocortical carcinoma was diagnosed.

Aldosterone-secreting tumors are rare but are most often reported in cats. Feline primary hyperaldosteronism (AKA **Conn's syndrome**) is an endocrine disorder characterized by the excessive, autonomous secretion of aldosterone from the adrenal cortex, most commonly caused by adrenal neoplasia. This primary hyperaldosteronism leads to hypokalemia and systemic hypertension. As in this case, hypokalemic polymyopathy is one of the most common presenting signs in cats with adrenal tumors causing hyperaldosteronism.



Figure 1. Formalin-fixed adrenocortical carcinoma in a 14-year-old cat. Distinctive cortex and medulla are replaced by a 2.5 cm x 2.0 cm x 1.1 cm soft, marbled light yellow to tan, encapsulated, rounded mass.

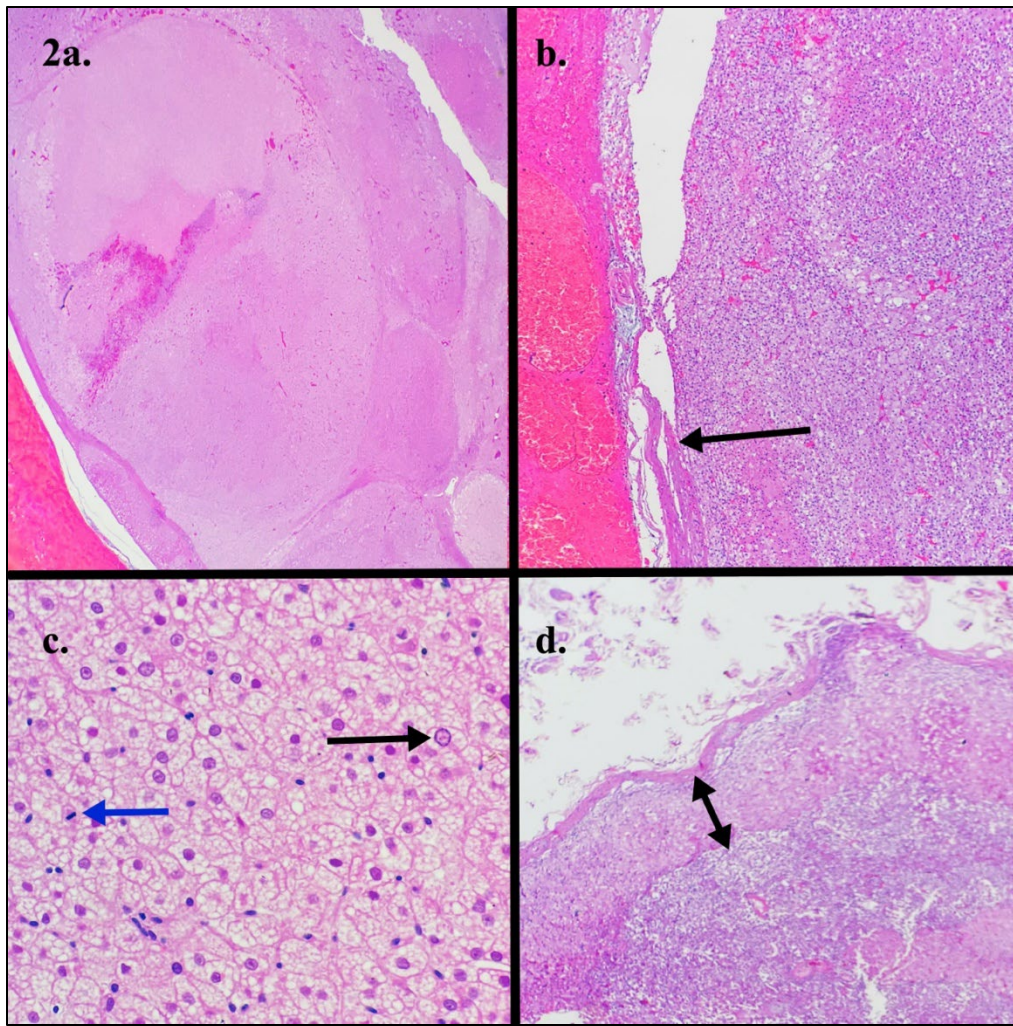


Figure 2. Histologic lesions of right adrenocortical carcinoma and left adrenal cortical atrophy. H&E stains. **a.** Right adrenal gland: multinodular masses replace the normal corticomedullary architecture. 4x. **b.** Right adrenal gland: neoplastic cells extend through the capsule (black arrow pointing to the fibrous capsule). 10x. **c.** Right adrenal gland: packeted, highly vacuolated neoplastic polygonal cells resembling epithelial cells of the adrenal cortex with a mitotic figure (blue arrow) and variation in nuclear size with some enlarged nuclei (black arrow). 20x. **d.** Left adrenal gland: a thinned (atrophic) contralateral cortex (double headed black arrow). 10x.

Reference

1. Rosol TJ, Grone A. Endocrine Glands. In: Jubb, Kennedy, and Palmer's Pathology of Domestic Animals, 7th ed. Maxie MG, ed. Elsevier, 2026; 1: 353-355.

Whole blood arsenic concentrations in cats: A diagnostic interpretation challenge

Felipe Reggeti, Jenny Tye

Animal Health Laboratory, University of Guelph, Guelph, ON (Reggeti); Derrydale Animal Hospital, Brampton, ON (Tye).

AHL Newsletter 2026;30(2):26.

A 6-year-old spayed female domestic short-haired (DSH) cat presented with a 3-week history of intermittent vomiting. The patient had been fed exclusively a commercial fish-only canned diet and was undergoing treatment for environmental allergies. Laboratory findings included increased SDMA, urea, and creatinine, and a urine specific gravity (USG) of 1.014, supporting renal disease; however, there was no evidence of proteinuria, and ultrasonographic examination of the kidneys and urinary tract was unremarkable.

Because of the fish-based diet, the owner expressed concern regarding heavy metal exposure, particularly mercury. EDTA blood samples were submitted to the toxicology section of the Animal Health Laboratory (AHL) for heavy metal analysis by ICP-MS. Blood mercury concentrations were 0.13 ppm and within the reference interval (RI: 0.10–0.30 ppm). However, the blood arsenic concentration was 0.72 ppm (720 ppb), exceeding proposed reference intervals of <0.05 ppm (50 ppb). This finding raised concerns regarding excessive arsenic exposure.

Arsenic occurs naturally in soil, and additional sources include coal, mining waste, seafood, well water, and some older pesticides and wood preservatives. Considering the clinical history, the fish-only diet was suspected as a possible source of arsenic exposure in this patient. To further assess exposure risk, feed samples were analyzed and compared with recommended maximum residue limits (MRLs) for arsenic in pet foods:

- U.S. Food and Drug Administration (US-FDA): 12.5 ppm (12,500 ppb)
- National Research Council (NRC): 30 ppm (30,000 ppb)

The arsenic concentration in the food was 0.92 ppm (920 ppb), which was within official recommendations. Since the cat had been fed this diet exclusively, the clinical significance of the presumably elevated blood arsenic concentration remained uncertain. To further evaluate arsenic concentrations in feline and canine blood, historical data from the AHL between 2016 and 2025 were reviewed (**Table 1**).

Table 1. Historical arsenic concentrations in whole blood of dogs and cats measured by ICP-MS at the AHL between 2016 and 2025.

Arsenic levels in anticoagulated blood (ppb)	Canine	Feline
# of submissions	n = 34	n =16
Minimum	1	16
Maximum	17	1000

Average	3.6	261.6
Median	1	110

These data show that circulating arsenic concentrations in feline whole blood are significantly higher than those observed in dogs. A previous study evaluating blood arsenic concentrations in domestic cats and other species reported similar findings. Based on this retrospective analysis, the authors suggested considering excessive arsenic exposure in cats when blood concentrations exceed 0.17 ppm (170 ppb). Similarly, most dogs in our retrospective dataset had very low or undetectable blood arsenic concentrations.

In the present case, the blood arsenic concentration of 0.72 ppm (720 ppb) fell within the historical range observed at the AHL (16–1000 ppb), although it exceeded previously proposed thresholds for excessive exposure in cats. Acute arsenic toxicosis typically produces gastrointestinal signs including vomiting, melena, diarrhea, and hypovolemia, whereas subacute cases may show tubular damage, azotemia, and potential renal failure. These findings appear consistent with the clinical presentation in this case. Furthermore, following a change to a different batch of the same food, the clinical signs and renal parameters progressively improved. However, a causal association with the suspect food could not be established because the arsenic concentration in the diet was low relative to established MRLs for arsenic in pet foods.

Research has shown that arsenic accumulates within rat erythrocytes to a greater extent than in other species. Rats rapidly methylate inorganic arsenic into a reactive dimethylated metabolite with a high affinity for hemoglobin, specifically the cysteine residue Cys13 on the α -chain. Binding at this site stabilizes the metabolite and promotes retention of arsenic within erythrocytes. Cats appear to exhibit a similar tendency for arsenic accumulation because feline hemoglobin also contains the cysteine α -13 residue, providing a comparable binding site for dimethylated arsenic metabolites. Therefore, **the relatively high arsenic concentrations observed in feline blood may reflect species-specific physiological characteristics of hemoglobin and may not necessarily indicate excessive arsenic exposure.** This phenomenon should be considered when interpreting laboratory results to avoid potential misinterpretation.

Blood arsenic concentrations in cats should therefore be interpreted in conjunction with clinical signs, other laboratory findings, and assessment of dietary intake.

References

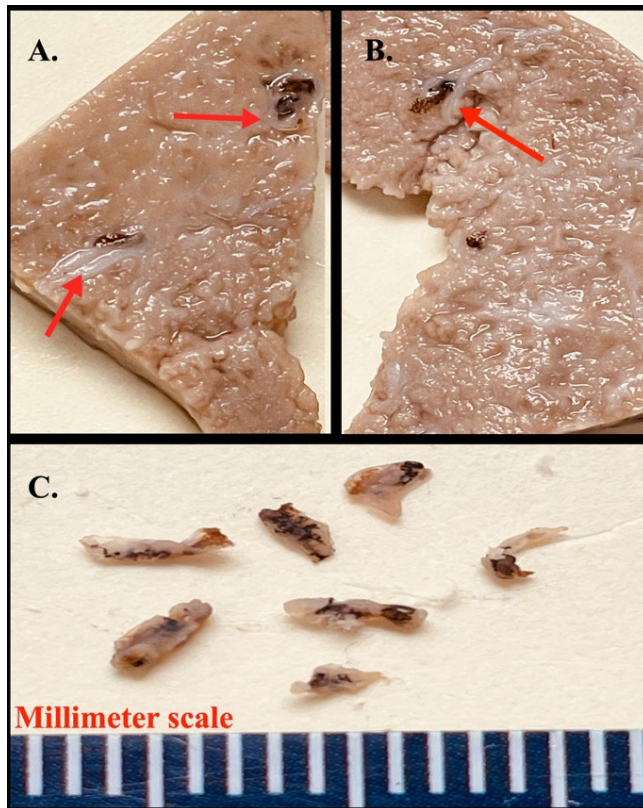
1. Puls, R. Mineral Levels in Animal Health: Diagnostic Data (2nd ed.). Sherpa International, Clearbrook, B.C. ISBN 0969342926, 1994.
2. U.S. Food and Drug Administration, Center for Veterinary Medicine. Target animal safety review memorandum, 2011. <https://www.fda.gov/media/81895/download>
3. National Research Council (US) Committee on Animal Nutrition. Mineral Tolerance of Animals. Washington (DC): National Academies Press; 2005.
4. Buchweitz JP, Drankhan HR, Lehner AF. Blood arsenic concentrations in felids. *Vet Rec* 2019;185(7):207.
5. Lu M, Wang H, Li XF, Arnold LL, Cohen SM, Le XC. Binding of dimethylarsinous acid to cys-13alpha of rat hemoglobin is responsible for the retention of arsenic in rat blood. *Chem Res Toxicol* 2007;20(1):27-37.

ANSWER: Dicrocoeliasis

Amanda Mansz

Animal Health Laboratory, University of Guelph, Guelph, ON.

AHL Newsletter 2026;30(2):28.



Figures 1A. & 1B. Formalin-fixed liver tissue from a 3-year-old ewe. Note the reduction of normal hepatic parenchyma and replacement with bands of intersecting fibrosis imparting a nodular appearance. Red arrows indicate bile ducts with periportal fibrosis and pigmented flukes within bile duct lumens.

Figure 1C. Darkly pigmented, 3 – 6 mm long fragments of adult flukes retrieved from bile duct lumens, consistent with *Dicrocoelium dendriticum* (AKA lancet liver fluke).

The lancet liver fluke lifecycle begins when embryonated eggs hatch after being swallowed by various genera of **land snails** (first intermediate host). Mother sporocysts produce a second generation of daughter sporocysts that produce cercariae that leave the snail in damp weather by being expelled from the snail's lung, clumped in a slime ball. The slime balls are swallowed by an **ant** (*Formica fusca* or other spp.) where the cercaria encyst, and the lifecycle is complete when the definitive host (the ewe in this case) swallows the ant. The route of larval migration through the definitive host is likely from the gut to the liver via the common bile duct where larvae mature and flukes begin laying eggs 10–12 weeks after infection. The total life cycle takes approximately 6 months. Infection in sheep is often considered incidental; however, the severity of the hepatic lesions is dependent on the number of parasites. Long-

standing heavy burdens can result in significant hepatic scarring. Typical histologic lesions are shown in (Fig. 2).

Dicrocoelium dendriticum can infect cattle, sheep and other ungulates. Infection of **alpacas and llamas** are more commonly associated with acute clinical decline. Rarely, **humans** (and other non-human primates) can be accidental definitive hosts.

Detection of eggs in feces using a flotation technique with a high specific gravity 1.30 to 1.45 is recommended. Preventing animals from grazing in the early morning or late evening, when ants are in tetany, and covering ant nests with tree branches to keep animals away from the base may also help reduce infections.

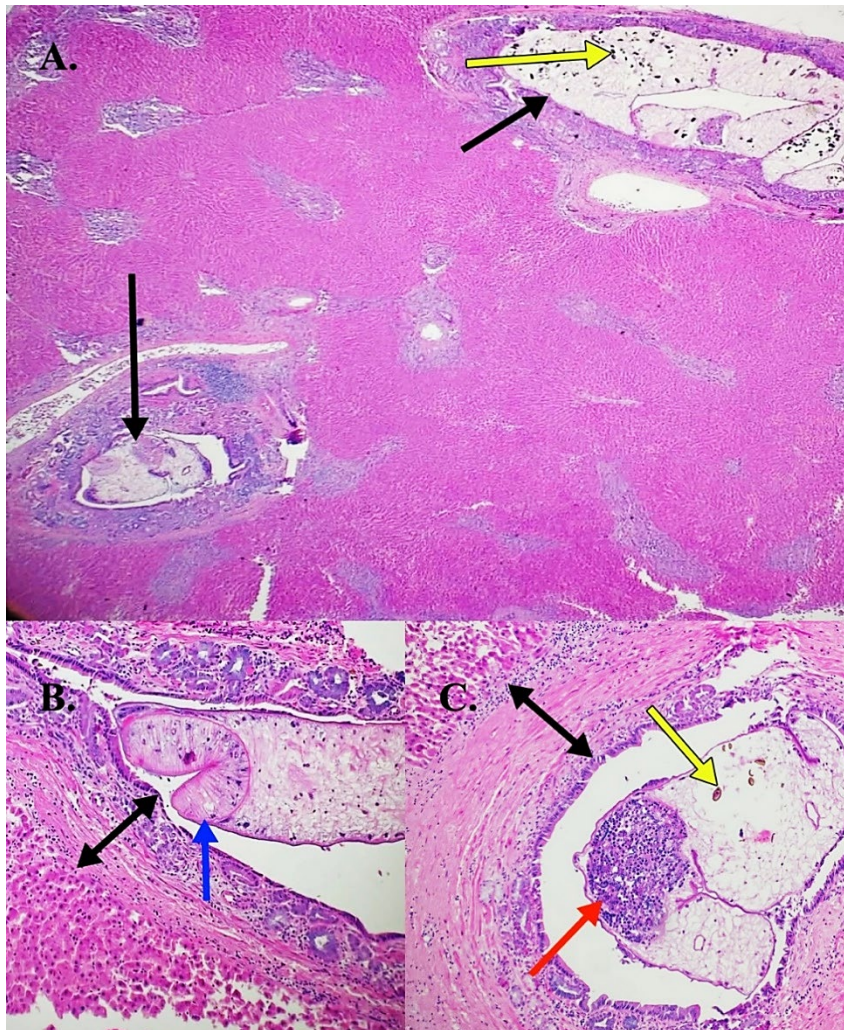


Figure 2. Histologic lesions induced in the liver by infection with the lancet liver fluke in a 3-year-old-ewe. H&E stain. **A.** Moderate periportal fibrosis and extensive biliary hyperplasia with adult flukes in bile ducts (black arrows). Dark brown pigmented eggs within the adult fluke present grossly as black discoloration in portal triads (yellow arrow). 10x. **B.** Bile duct surrounded by biliary hyperplasia and fibrosis (double-headed arrow) containing an adult fluke with a prominent sucker (blue arrow) in the bile duct lumen. 20x. **C.** Bile duct surrounded by biliary hyperplasia and fibrosis (double-headed arrow) with an adult fluke (red arrow) and dark brown pigmented eggs (yellow arrow) within the bile duct lumen. 20x.

an adult fluke with testis and sperm (red arrow) and dark brown pigmented operculated eggs (yellow arrow). 20x.

Reference

1. Cullen JM, Van Wettere AJ. Liver and Biliary System. In: Jubb, Kennedy, and Palmer's Pathology of Domestic Animals, 7th ed. Maxie MG, ed. Elsevier, 2026;2:325.